

Exotic Magnetism on the Quasi-fcc Lattices of the d^3 Double Perovskites $\text{La}_2\text{NaB}'\text{O}_6$ ($B' = \text{Ru}, \text{Os}$)

A. A. Aczel,^{1,*} P. J. Baker,² D. E. Bugaris,³ J. Yeon,³ H.-C. zur Loye,³ T. Guidi,² and D. T. Adroja^{2,4}

¹Quantum Condensed Matter Division, Oak Ridge National Laboratory, Oak Ridge, Tennessee 37831, USA

²ISIS Facility, STFC Rutherford Appleton Laboratory, Harwell Oxford, Oxfordshire OX11 0QX, United Kingdom

³Department of Chemistry and Biochemistry, University of South Carolina, Columbia, South Carolina 29208, USA

⁴Physics Department, University of Johannesburg, P.O. Box 524, Auckland Park 2006, South Africa

(Received 7 January 2014; published 20 March 2014)

We find evidence for long-range and short-range ($\zeta = 70 \text{ \AA}$ at 4 K) incommensurate magnetic order on the quasi-face-centered-cubic (fcc) lattices of the monoclinic double perovskites $\text{La}_2\text{NaRuO}_6$ and $\text{La}_2\text{NaOsO}_6$, respectively. Incommensurate magnetic order on the fcc lattice has not been predicted by mean field theory, but may arise via a delicate balance of inequivalent nearest neighbor and next nearest neighbor exchange interactions. In the Ru system with long-range order, inelastic neutron scattering also reveals a spin gap $\Delta \sim 2.75 \text{ meV}$. Magnetic anisotropy is generally minimized in the more familiar octahedrally coordinated $3d^3$ systems, so the large gap observed for $\text{La}_2\text{NaRuO}_6$ may result from the significantly enhanced value of spin-orbit coupling in this $4d^3$ material.

DOI: 10.1103/PhysRevLett.112.117603

PACS numbers: 76.30.He, 71.70.Ej, 75.25.-j, 76.75.+i

There has been a plethora of recent interest in B -site ordered double perovskites (DPs) with the formula $A_2BB'\text{O}_6$. When magnetic atoms only occupy the B' sites and nearest-neighbor (NN) antiferromagnetic (AFM) coupling is dominant, all the exchange interactions cannot be satisfied simultaneously and geometric frustration on the face-centered cubic (fcc) lattice is realized. Since the B' sites can accommodate a wide variety of magnetic ions, DPs are particularly attractive for systematic magnetic studies of frustrated fcc systems where one can tune either the d electron configuration or the spin-orbit coupling (SOC).

A wide range of magnetic ground states have been predicted theoretically in $4d$ and $5d$ DPs with d^1 and d^2 electronic configurations [1,2]. Several exotic magnetic ground states have also been observed experimentally, including a collective singlet state which has been described as a valence bond glass in Ba_2YMoO_6 [3–5], spin freezing without long-range order in Ba_2YReO_6 [6], $\text{Sr}_2\text{MgReO}_6$ [7], and $\text{Sr}_2\text{CaReO}_6$ [8], a ferromagnetic (FM) Mott-insulating state in $\text{Ba}_2\text{NaOsO}_6$ [9,10], and the $J_{\text{eff}} = 1/2$ Mott-insulating state in the iridates $\text{La}_2\text{MgIrO}_6$ and $\text{La}_2\text{ZnIrO}_6$ [11].

In the context of the interplay between geometric frustration and SOC, there has been less interest in $4d$ and $5d$ DPs with the electronic configuration d^3 . One downside is that d^3 systems are generally assumed to possess spin-only $S = 3/2$ ground states with quenched orbital angular momentum according to the usual L - S coupling scheme, since the magnetic B' ions are in a local octahedral environment, and this configuration should minimize the effects of SOC.

Another issue is d^3 DP systems are expected to behave more classically due to the large spins, and for almost all known cases long-range magnetic order is found [12].

Although magnetic order cannot be stabilized on the fcc lattice solely by NN AFM exchange interactions $J_1 > 0$, finite next-nearest-neighbor (NNN) exchange J_2 or magnetic anisotropy can alleviate the classical ground state degeneracy [13] and allow the systems to order. The phase diagram of the J_1 - J_2 model has been determined theoretically for the fcc lattice using mean field theory (MFT) [14,15]. Four different collinear magnetic phases are found, including ferromagnetism and type I, type II, and type III antiferromagnetism. All four phases have been realized in d^3 and d^5 DPs, with type I and type II AFM especially common (e.g., see Refs. [16–23]). On the other hand, type III AFM and ferromagnetic (FM) order are rare, but they have been found in the systems $\text{Ba}_2\text{LaRuO}_6$ [16] and $\text{Ca}_2\text{SbCrO}_6$ [24], respectively.

Recently, we investigated the magnetism of the monoclinic d^3 DPs $\text{La}_2\text{NaRuO}_6$ and $\text{La}_2\text{NaOsO}_6$ by magnetic susceptibility, heat capacity, and neutron powder diffraction [25]. The magnetic susceptibility shows a deviation from the Curie-Weiss law ($\theta_{\text{CW}} = -57 \text{ K}$) at 15 K for $\text{La}_2\text{NaRuO}_6$, accompanied by a λ anomaly in the specific heat at the same temperature. While the magnetic susceptibility of $\text{La}_2\text{NaOsO}_6$ shows a similar deviation from Curie-Weiss law behavior ($\theta_{\text{CW}} = -74 \text{ K}$) around 12 K, only a broad feature is observed in the specific heat. Furthermore, contrary to expectations from the MFT phase diagram, we found incommensurate long-range order in $\text{La}_2\text{NaRuO}_6$ and no magnetic Bragg peaks for $\text{La}_2\text{NaOsO}_6$ down to 4 K [25]. This behavior is difficult to understand in the general context of d^3 DPs.

In this Letter, we have investigated these d^3 systems with muon spin relaxation (μSR) and time-of-flight neutron scattering measurements. μSR allows for a careful study of the T dependence of the magnetism in these materials,

while neutron scattering is useful for understanding detailed information on the nature of the magnetic ground states and spin dynamics. Our study confirms incommensurate long-range magnetic order in $\text{La}_2\text{NaRuO}_6$ with $T_N = 15(1)$ K and reveals short-range incommensurate order in $\text{La}_2\text{NaOsO}_6$ down to 4 K with a correlation length $\zeta = 70$ Å. These two systems have large monoclinic β angles relative to most other B -site ordered, d^3 DPs [25]. While the local cubic symmetry and the ideal fcc sublattice of the magnetic B' ions remain nearly intact in monoclinic systems, the resulting structural distortions can induce substantial tilting of the BO_6 and $B'\text{O}_6$ octahedra, leading to significantly altered NN B' -O- B' and NNN B' -O- B -O- B' exchange interactions [23,25]. This effect seems to push $\text{La}_2\text{NaRuO}_6$ and $\text{La}_2\text{NaOsO}_6$ to the MFT phase boundary between type I and type III AFM.

For the $\text{La}_2\text{NaRuO}_6$ system with long-range magnetic order, we find a sizable spin gap $\Delta \sim 2.75$ meV in the excitation spectrum. Recent neutron work has also found spin gaps in several other ordered $4d^3$ and $5d^3$ cubic and monoclinic DPs. We find that the gaps roughly scale with T_N , suggesting a common origin. Any plausible explanation should be based on the intermediate-to-large SOC expected in these systems. The two most likely scenarios are related to symmetric exchange anisotropy or the breakdown of L - S coupling in these $4d^3$ and $5d^3$ materials. The latter could lead to a significantly unquenched orbital moment.

To perform the present study, polycrystalline $\text{La}_2\text{NaRuO}_6$ and $\text{La}_2\text{NaOsO}_6$ were prepared according to the procedure in Refs. [25–27]. For the μSR experiments [28], 2 g of each sample were measured on the EMU spectrometer, in longitudinal geometry, at the ISIS Pulsed Neutron and Muon Source, United Kingdom. The neutron scattering measurements were carried out on the MERLIN [29] and LET [30] time-of-flight chopper spectrometers at ISIS. Data was collected on 15 g powder samples with a neutron energy E_i of 10 meV.

Typical zero-field (ZF) μSR data for $\text{La}_2\text{NaRuO}_6$ and $\text{La}_2\text{NaOsO}_6$ are shown in Figs. 1(a) and 1(b). There is a clear drop in the initial asymmetry on cooling below $T_N = 15$ K and 6 K for the Ru and Os systems, respectively, as shown in Fig. 1(c). This implies that internal fields larger than those that can be resolved at ISIS (~ 80 mT) are present in both samples at low temperature. To model the T dependence of the muon data we used the function: $A(t) = A_0 e^{-(\lambda t)^\beta} + A_1$, where A_0 represents the amplitude of the relaxing signal, λ is the muon spin relaxation rate, β reflects the type of field distribution in the sample, and A_1 is a nonrelaxing component only required for the Ru case at low T .

For the Ru system, the drop in initial asymmetry is accompanied by the development of a nonrelaxing A_1 component, as illustrated in Fig 1(d). In the ordered state, the muons that experience a quasistatic local field along their spin direction do not precess and therefore give rise to this nonrelaxing component. The decrease in the initial asymmetry is also coincident with an increase in λ and an

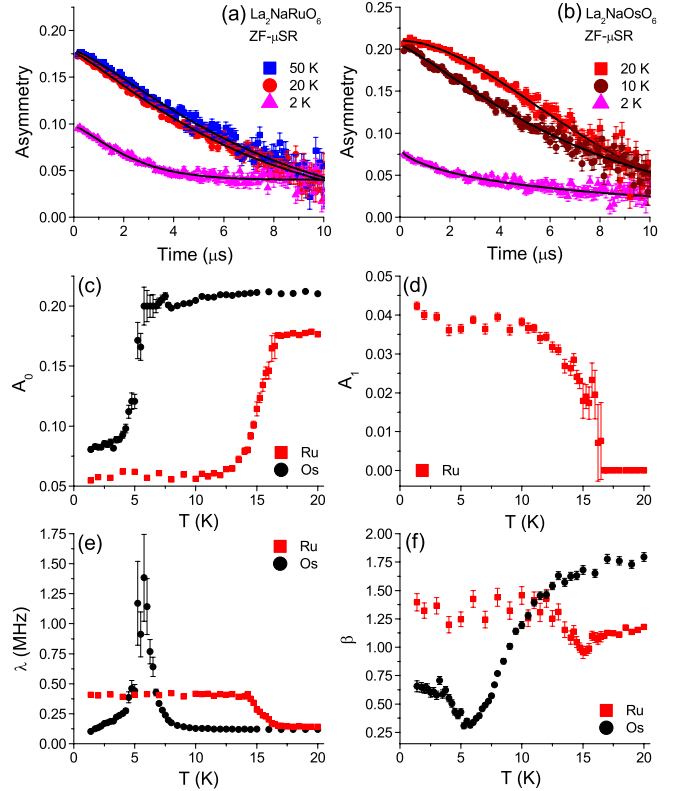


FIG. 1 (color online). ZF- μSR measurements of $\text{La}_2\text{NaRuO}_6$ and $\text{La}_2\text{NaOsO}_6$. (a),(b) Asymmetry vs time at selected temperatures for the Ru and Os systems, respectively. (c) T dependence of the asymmetry A_0 for both systems. (d) T dependence of A_1 for the Ru system. (e),(f) T dependence of the relaxation rate λ and power β for both systems.

abrupt change in β , as displayed in Figs. 1(e) and 1(f). The increase in λ with decreasing T is likely caused by the broad distribution of static local fields found in the long-range incommensurate state.

For the Os system, as shown in Fig. 1(e), the ZF-relaxation rate peaks at 6 K. This does not correspond to the 12 K ordering temperature inferred from the magnetic susceptibility and specific heat [25]. Also, Fig. 1(f) shows that β begins to decrease significantly below 12 K, dropping to around $1/3$ at 6 K before recovering to $\sim 2/3$ at 1.5 K. This is not normal behavior for a system entering a long-range ordered state, and instead suggests that the Os spins are slowing down gradually and freezing below $T_f = 6$ K.

Time-of-flight neutron scattering provides complementary information to the μSR study. Data from MERLIN in the elastic channel with $E_i = 10$ meV is shown for $\text{La}_2\text{NaRuO}_6$ in Fig. 2(a), and reveals resolution-limited, incommensurate Bragg peaks at $Q \sim 0.72$ Å $^{-1}$ and 0.86 Å $^{-1}$ in agreement with observations from Ref. [25]. These peaks disappear at T_N and give way to diffuse scattering that decreases gradually with increasing temperature. A 16–100 K difference plot of the scattering is shown in Fig. 2(c). The shape of the diffuse scattering is characteristic of a Warren line

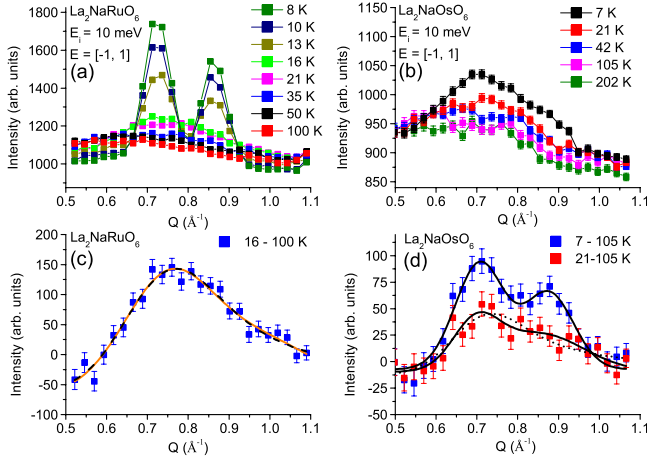


FIG. 2 (color online). Elastic neutron scattering intensity for $\text{La}_2\text{NaRuO}_6$ and $\text{La}_2\text{NaOsO}_6$ from MERLIN with $E_i = 10$ meV integrated over ± 1 meV. (a),(b) T dependence of the scattering at selected temperatures for the Ru and Os systems, respectively. (c) Diffuse scattering observed at 16 K for $\text{La}_2\text{NaRuO}_6$ with a background at 100 K subtracted. (d) Diffuse scattering at 7 and 21 K for $\text{La}_2\text{NaOsO}_6$ with a background at 105 K subtracted. The solid and dashed curves shown in (c) and (d) are fits described in the text.

shape for 2D magnetic correlations [31,32]. Short range order of this type has been reported for the fcc systems Sr_2YRuO_6 [33] and GdInCu_4 [34], and 2D magnetic fluctuations have been predicted theoretically for the frustrated fcc lattice in general [35]. These past results suggest that 2D magnetism may be a defining feature of this particular lattice, and therefore we consider a Warren line shape analysis of our $\text{La}_2\text{NaRuO}_6$ data.

The dashed black curve in Fig. 2(c) is a fit to a Warren line shape with $Q_0 = 0.73 \text{ \AA}^{-1}$ and a correlation length $\zeta = 25 \text{ \AA}$. The position of maximum scattering intensity Q_0 should correspond to the (hk) indices of the Bragg rod giving rise to the 2D correlations. Since the closest commensurate reflections to Q_0 are $(0.5, 0.5)_{hl}$ and $(01)_{hl}$ with $Q \sim 0.70 \text{ \AA}^{-1}$ and 0.79 \AA^{-1} , respectively, a Warren line shape does not seem to explain the diffuse scattering. Another possibility is that the diffuse scattering is composed of two incommensurate magnetic peaks that are not resolution limited. To estimate ζ in this case, the diffuse scattering in Fig. 2(c) was fit to two Gaussian functions (solid orange curve). The correlation length was then calculated using $\zeta = 2\pi / \sqrt{F_M^2 - F_N^2}$, where F_M and F_N are the full-width half maximums (FWHM) of the magnetic and nuclear peaks respectively. A value of $\zeta = 20 \text{ \AA}$ at 16 K is obtained by this method.

Elastic neutron scattering results are shown in Figs. 2(b) and 2(d) for $\text{La}_2\text{NaOsO}_6$. No resolution-limited magnetic Bragg peaks are observed down to 7 K, but similar diffuse scattering is observed. The dashed black curve in Fig. 2(d) shows that in principle the 21–105 K Os diffuse scattering can be fit to a Warren line shape, and in this case $\zeta = 30 \text{ \AA}$

and $Q_0 = 0.70 \text{ \AA}^{-1}$, corresponding to a $(0.5, 0.5)_{hl}$ Bragg rod. However, this data can be fit equally well to two broad incommensurate Gaussian peaks (solid black curve) centered about the (001) Bragg position. Using the formula for ζ given above, this model yields $\zeta = 35 \text{ \AA}$. The diffuse scattering becomes two well-defined incommensurate peaks below $T^* = 12 \text{ K}$, but a finite correlation length of $\zeta = 50 \text{ \AA}$ remains even at 7 K.

The magnetic ground states of $\text{La}_2\text{NaRuO}_6$ and $\text{La}_2\text{NaOsO}_6$ are not predicted by MFT. Considering the theoretical J_1 - J_2 phase diagram for fcc magnets given in Ref. [15], one possible explanation is these systems are on the border between type I and type III AFM. The phase boundary corresponds to NN $J_1 > 0$ and a NNN $J_2 = 0$. This situation presumably arises due to the large tilting of the NaO_6 and $B'\text{O}_6$ octahedra weakening the ferromagnetic J_2 interactions necessary for type I AFM. This scenario is more likely than the systems lying on the border between FM and type I AFM, since they are highly frustrated (not expected for $J_1 = 0$ and $J_2 < 0$) and possess large, negative θ_{CW} 's. We do not consider placing $\text{La}_2\text{NaRuO}_6$ and $\text{La}_2\text{NaOsO}_6$ on the other phase boundaries, as $\text{La}_2\text{LiRuO}_6$ with a smaller monoclinic distortion is type I AFM [19], and in general most Ru^{5+} and Os^{5+} DPs are type I AFM.

Color maps of the neutron scattering spectra are shown in Figs. 3(a)–3(c) for $\text{La}_2\text{NaRuO}_6$ at selected temperatures.

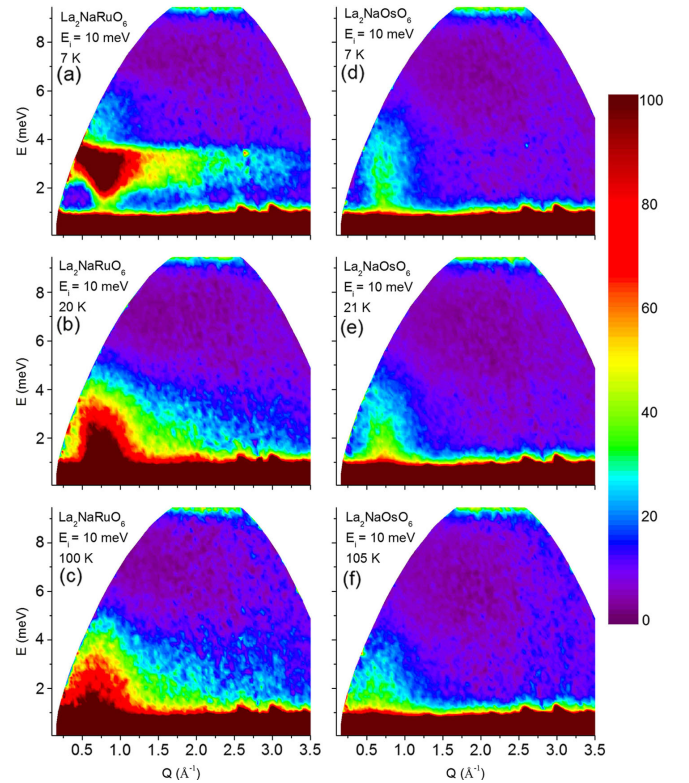


FIG. 3 (color online). Neutron scattering spectra for (a)–(c) $\text{La}_2\text{NaRuO}_6$ and (d)–(f) $\text{La}_2\text{NaOsO}_6$ at selected temperatures from MERLIN with $E_i = 10$ meV.

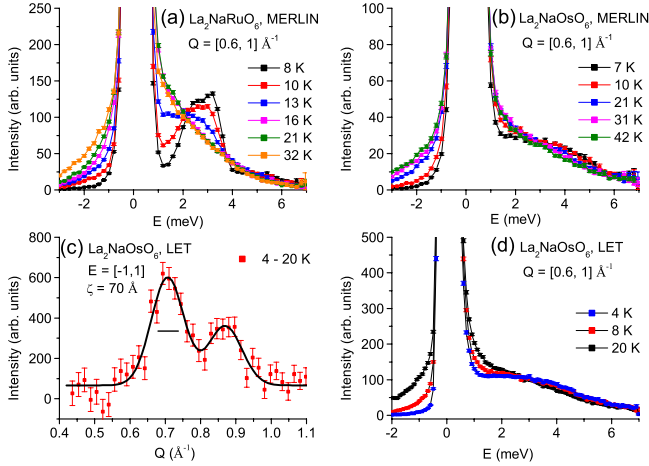


FIG. 4 (color online). Scattering intensity vs energy transfer from MERLIN with $E_i = 10$ meV, integrated over $0.6 < Q < 1 \text{ \AA}^{-1}$ for (a) $\text{La}_2\text{NaRuO}_6$ and (b) $\text{La}_2\text{NaOsO}_6$. (c) Difference plot of elastic neutron scattering data for $\text{La}_2\text{NaOsO}_6$, integrated over $-1 < E < 1$, from LET with $E_i = 10$ meV. Instrumental Q resolution is indicated by the horizontal line. (d) Scattering intensity vs energy transfer, integrated over $0.6 < Q < 1 \text{ \AA}^{-1}$, for $\text{La}_2\text{NaOsO}_6$ from LET with $E_i = 10$ meV.

Below T_N , we observe gapped, dispersive spin wave excitations. Following previous convention in the literature for powder samples [36,37], where the gap Δ has been associated with the center of mass of the acoustic mode near the magnetic zone center, we estimate $\Delta \sim 2.75$ meV. The T evolution of the spin gap is illustrated more clearly in Fig. 4(a), which shows the energy dependence of the Q -integrated scattering around the incommensurate $Q = 0.72 \text{ \AA}^{-1}$ and 0.86 \AA^{-1} positions ($0.6 < Q < 1 \text{ \AA}^{-1}$). The observation of a spin gap with a magnitude larger than T_N in an octahedrally coordinated d^3 , 3D system is highly unusual. For the more familiar case of $3d^3$ systems, a combination of strong crystal fields and negligible SOC generally ensure that the magnetic anisotropy is minimal.

Additional insight on the origin of the spin gap for $\text{La}_2\text{NaRuO}_6$ comes from direct comparison to the spin gaps observed for other cubic and monoclinic DPs. The cubic $4d^3$ system Ba_2YRuO_6 ($T_N = 36$ K) has $\Delta = 5$ meV [36], the cubic $5d^3$ system Ba_2YOsO_6 ($T_N = 70$ K) has $\Delta = 15$ meV [38], and the monoclinic $4d^3$ system Sr_2YRuO_6 ($T_N = 24$ K) has $\Delta = 5$ meV [39]. The transition temperatures and gap sizes seem to roughly scale with one another, suggesting a common origin. The cubic crystal fields for Ru^{5+} and Os^{5+} in Ba_2YRuO_6 and Ba_2YOsO_6 , combined with the quenched orbital angular momentum expected from the L - S coupling scheme, rule out single ion anisotropy as an origin of the spin gap in those cases [40]. The high cubic symmetry of these two compounds also eliminates the Dzyaloshinsky-Moriya (DM) interaction from consideration.

Symmetric exchange anisotropy is a second-order SOC effect involving the excited states of two magnetic ions, and

therefore usually much weaker compared to single ion anisotropy and the DM interaction. However, it can play an important role in the magnetic anisotropy of $4d^3$ and $5d^3$ DPs [13], where these other effects are minimized and SOC is significant. In fact, recent work on monoclinic Sr_2YRuO_6 has shown that the gapped magnetic excitation spectrum can be explained well with a model that includes NN symmetric exchange anisotropy [39]. Furthermore, this effect cannot be ruled out even in the case of ideal fcc magnetic sublattices [41], and therefore could be the primary spin gap mechanism in all these DPs.

On the other hand, the spin gaps may arise from the breakdown of L - S coupling in these $4d$ and $5d$ systems. Recent theoretical work [42] shows that SOC values typical of $4d$ and $5d$ transition metals, combined with reduced intra-Coulomb interactions due to the extended orbitals, lead to an unquenched orbital moment and magnetic anisotropy in octahedrally coordinated $4d^3$ and $5d^3$ systems. These findings can be understood as a tendency towards j - j coupling for these materials, where the ground states for the heavy magnetic ions are not governed by Hund's rules, but instead arise from coupled total angular momentum (orbital and spin) of their individual electrons.

In contrast to $\text{La}_2\text{NaRuO}_6$, a spin gap never fully develops below T_f down to 4 K for $\text{La}_2\text{NaOsO}_6$, as indicated with combined MERLIN and LET data presented in Figs. 3(d)–3(f) and Figs. 4(b) and 4(d). The LET data in Fig. 4(c) shows that the lack of a well-defined spin gap coincides with the short-range order persisting down to 4 K ($\zeta = 70 \text{ \AA}$). These observations further illustrate that the gapped excitations in $4d^3$ and $5d^3$ DPs can be associated directly with the long-range order, and therefore are not expected to be a defining feature in the Os system.

In conclusion, muon spin relaxation and neutron scattering measurements find evidence for long-range and short-range incommensurate magnetic order on the quasi-fcc lattices of $\text{La}_2\text{NaRuO}_6$ and $\text{La}_2\text{NaOsO}_6$, respectively. These magnetic states may arise due to a delicate balance of exchange interactions induced by the large tilting of the NaO_6 and $B'\text{O}_6$ octahedra. Furthermore, in the Ru d^3 system with long-range order, inelastic neutron scattering reveals a spin gap $\Delta \sim 2.75$ meV. The values of T_N and the magnitude of the gaps in ordered $4d^3$ and $5d^3$ DPs seem to exhibit nearly linear scaling behavior, suggesting a common origin. We propose that these spin gaps arise as a consequence of the intermediate-to-large SOC in these materials, through either symmetric anisotropic exchange or the breakdown of L - S coupling. X-ray magnetic circular dichroism measurements on $4d^3$ and $5d^3$ cubic DPs are essential to distinguish between these two possibilities.

We acknowledge B. D. Gaulin, J. P. Clancy, and J. P. Carlo for useful discussions. This research was supported by the U.S. Department of Energy, Office of Basic Energy Sciences. A. A. A. was supported by the Scientific User Facilities Division. D. E. B. and H. z. L. would like to

acknowledge financial support through the Heterogeneous Functional Materials for Energy Systems (HeteroFoaM) Energy Frontiers Research Center (EFRC), funded by the U.S. Department of Energy, Office of Basic Energy Sciences under Award No. DE-SC0001061.

*Corresponding author.
aczela@ornl.gov

- [1] G. Chen, R. Pereira, and L. Balents, *Phys. Rev. B* **82**, 174440 (2010).
- [2] G. Chen and L. Balents, *Phys. Rev. B* **84**, 094420 (2011).
- [3] T. Aharen, J.E. Greedan, C.A. Bridges, A.A. Aczel, J. Rodriguez, G.J. MacDougall, G.M. Luke, T. Imai, V.K. Michaelis, S. Kroeker, H.D. Zhou, C.R. Wiebe, and L.M.D. Cranswick, *Phys. Rev. B* **81**, 224409 (2010).
- [4] J.P. Carlo, J.P. Clancy, T. Aharen, Z. Yamani, J.P.C. Ruff, J.J. Wagman, G.J. Van Gastel, H.M.L. Noad, G.E. Granroth, J.E. Greedan, H.A. Dabkowska, and B.D. Gaulin, *Phys. Rev. B* **84**, 100404(R) (2011).
- [5] M.A. de Vries, A.C. McLaughlin, and J.W.G. Bos, *Phys. Rev. Lett.* **104**, 177202 (2010).
- [6] T. Aharen, J.E. Greedan, C.A. Bridges, A.A. Aczel, J. Rodriguez, G.J. MacDougall, G.M. Luke, V.K. Michaelis, S. Kroeker, C.R. Wiebe, H.D. Zhou, and L.M.D. Cranswick, *Phys. Rev. B* **81**, 064436 (2010).
- [7] C.R. Wiebe, J.E. Greedan, P.P. Kyriakou, G.M. Luke, J.S. Gardner, A. Fukaya, I.M. Gat-Malureanu, P.L. Russo, A.T. Savici, and Y.J. Uemura, *Phys. Rev. B* **68**, 134410 (2003).
- [8] C.R. Wiebe, J.E. Greedan, G.M. Luke, and J.S. Gardner, *Phys. Rev. B* **65**, 144413 (2002).
- [9] K.E. Stitzer, M.D. Smith, and H.-C. zur Loye, *Solid State Sci.* **4**, 311 (2002).
- [10] A.S. Erickson, S. Misra, G.J. Miller, R.R. Gupta, Z. Schlesinger, W.A. Harrison, J.M. Kim, and I.R. Fisher, *Phys. Rev. Lett.* **99**, 016404 (2007).
- [11] G. Cao *et al.*, *Phys. Rev. B* **87**, 155136 (2013).
- [12] J.E. Greedan, S. Derakhshan, F. Ramezanipour, J. Siewenie, and Th. Proffen, *J. Phys. Condens. Matter* **23**, 164213 (2011).
- [13] E.V. Kuz'min, S.G. Ovchinnikov, and D.J. Singh, *Phys. Rev. B* **68**, 024409 (2003).
- [14] D. ter Harr and M.E. Lines, *Phil. Trans. R. Soc. A* **254**, 521 (1962); **255**, 1 (1962).
- [15] K. Lefmann and C. Rischel, *Eur. Phys. J. B* **21**, 313 (2001).
- [16] P.D. Battle, J.B. Goodenough, and R. Price, *J. Solid State Chem.* **46**, 234 (1983).
- [17] P.D. Battle and W.J. Macklin, *J. Solid State Chem.* **52**, 138 (1984).
- [18] P.D. Battle and C.W. Jones, *J. Solid State Chem.* **78**, 108 (1989).
- [19] P.D. Battle, C.P. Grey, M. Hervieu, C. Martin, C.A. Moore, and Y. Paik, *J. Solid State Chem.* **175**, 20 (2003).
- [20] L. Ortega-San Martin, J.P. Chapman, L. Lezama, J.S. Marcos, J. Rodriguez-Fernandez, M.I. Arriortua, and T. Rojo, *Eur. J. Inorg. Chem.* **2006**, 1362 (2006).
- [21] A.A. Aczel, D.E. Bugaris, J. Yeon, C. de la Cruz, H.C. zur Loye, and S.E. Nagler, *Phys. Rev. B* **88**, 014413 (2013).
- [22] A. Munoz, J.A. Alonso, M.T. Casais, M.J. Martinez-Lope, and M.T. Fernandez-Diaz, *J. Phys. Condens. Matter* **14**, 8817 (2002).
- [23] J.-W.G. Bos and J.P. Attfield, *Phys. Rev. B* **70**, 174434 (2004).
- [24] M. Retuerto, M. Garcia-Hernandez, M.J. Martinez-Lope, M.T. Fernandez-Diaz, J.P. Attfield, and J.A. Alonso, *J. Mater. Chem.* **17**, 3555 (2007).
- [25] A.A. Aczel, D.E. Bugaris, L. Li, J.-Q. Yan, C. de la Cruz, H.C. zur Loye, and S.E. Nagler, *Phys. Rev. B* **87**, 014435 (2013).
- [26] W.R. Gemmill, M.D. Smith, and H.-C. zur Loye, *J. Solid State Chem.* **177**, 3560 (2004).
- [27] W.R. Gemmill, M.D. Smith, R. Prozorov, and H.-C. zur Loye, *Inorg. Chem.* **44**, 2639 (2005).
- [28] S.J. Blundell, *Contemp. Phys.* **40**, 175 (1999).
- [29] R.I. Bewley, R.S. Eccleston, K.A. McEwen, S.M. Hayden, M.T. Dove, S.M. Bennington, J.R. Treadgold, and R.L.S. Coleman, *Physica (Amsterdam)* **385B–386B**, 1029 (2006).
- [30] R.I. Bewley, J.W. Taylor, and S.M. Bennington, *Nucl. Instrum. Methods Phys. Res., Sect. A* **637**, 128 (2011).
- [31] H. Zhang, J.W. Lynn, W.-H. Li, T.W. Clinton, and D.E. Morris, *Phys. Rev. B* **41**, 11 229 (1990).
- [32] A.S. Wills, N.P. Raju, C. Morin, and J.E. Greedan, *Chem. Mater.* **11**, 1936 (1999).
- [33] E. Granado, J.W. Lynn, R.F. Jardim, and M.S. Torikachvili, *Phys. Rev. Lett.* **110**, 017202 (2013).
- [34] H. Nakamura, N. Kim, M. Shiga, R. Kmiec, K. Tomala, E. Ressouche, J.P. Sanchez, and B. Malaman, *J. Phys. Condens. Matter* **11**, 1095 (1999).
- [35] S. Alexander and P. Pincus, *J. Phys. A* **13**, 263 (1980).
- [36] J.P. Carlo, J.P. Clancy, K. Fritsch, C.A. Marjerrison, G.E. Granroth, J.E. Greedan, H.A. Dabkowska, and B.D. Gaulin, *Phys. Rev. B* **88**, 024418 (2013).
- [37] S. Lee, J.-G. Park, D.T. Adroja, D. Khomskii, S. Streltsov, K.A. McEwen, H. Sakai, K. Yoshimura, V.I. Anisimov, D. Mori, R. Kanno, and R. Ibberson, *Nat. Mater.* **5**, 471 (2006).
- [38] B.D. Gaulin *et al.* (to be published).
- [39] D.T. Adroja, J. Paddison, R. Singh, C.V. Tomy, M. Rotter, P. Deen, W. Kockleman, M. Koza, J.R. Stewart, and A. Goodwin (to be published).
- [40] D. Alders, R. Coehoorn, and W.J.M. de Jonge, *Phys. Rev. B* **63**, 054407 (2001).
- [41] B. Halg and A. Furrer, *Phys. Rev. B* **34**, 6258 (1986).
- [42] H. Matsuura and K. Mityake, *J. Phys. Soc. Jpn.* **82**, 073703 (2013).